Evaluating and Increasing the Renewable Energy Share of Customers' Electricity Consumption

SHUAI FAN[1], (Student Member, IEEE), **ZHENGSHUO LI**[2], (Member, IEEE),
ZUYI LI[3], (Senior Member, IEEE), AND **GUANGYU HE**[1], (Senior Member, IEEE)

[1]Key Laboratory of Control of Power Transmission and Conversion, Ministry of Education, Shanghai Jiao Tong University, Shanghai 200240, China
[2]School of Electrical Engineering, Shandong University, Jinan 250000, China
[3]Galvin Center for Electricity Innovation, Illinois Institute of Technology, Chicago, IL 60616, USA

Corresponding author: Guangyu He (gyhe@sjtu.edu.cn)

ABSTRACT Demand response (DR) is a critical enabler for promoting the integration of significant renewable energy sources (RES) into power systems. However, the contribution of each customer to the amount of integrated RES in the entire system cannot be quantified based on current studies, which hinders the deployment and promotion of DR programs. To address this problem, an index to quantitatively evaluate the marginal impact on the amount of integrated RES in the whole system caused by a customer (MIR) was proposed in this paper. The MIR proved to be reasonable for the evaluation of the renewable energy share of a customer's electricity consumption (RSC). We subsequently proposed an RSC-based DR scheme, in which customers are motivated to individually reshape their load profiles to obtain a higher RSC, which accordingly facilitates integrating RES in the whole system. Optimal load reshaping strategies were derived from a bilevel optimization model, which was converted into a mathematical program with primal and dual constraints (MPPDC). The test system was generated based on the load data from Open Energy Information and RES data from the PJM. We corroborated the RSC evaluation result analytically and numerically. Further tests on the RSC-based DR scheme showed it could help facilitate integrating considerably more RES into the power system.

INDEX TERMS Demand response, renewable energy sources, marginal impact, MPDDC.

NOMENCLATURE

ABBREVIATIONS AND DEFINITIONS

RES	Renewable energy sources
CBL	Customer baseline load
LSE	Load services entity
HEMS	Home energy management system
MIR	Marginal impact on the amount of integrated RES in the whole system caused by a customer
MIB	Marginal impact on the power balancing burden for conventional units caused by a customer
RSC	Renewable energy share of a customer's daily electricity consumption
RSS	Renewable energy share of the system-level consumption per time slot
DRSS	Daily renewable energy share of the system-level electricity consumption
M-DRSS	Maximal available DRSS

The associate editor coordinating the review of this manuscript and approving it for publication was Bin Zhou.

SETS

$\mathcal{T}$	Time slots set indexed by t, with the cardinality of T
$\mathcal{T}_{-1}$	$\mathcal{T}_{-1} := \{2, 3, \ldots, T\}$
$\mathcal{I}$	Customer set indexed by i, with the cardinality of I
$\mathcal{J}$	Typical load profiles indexed by j, with the cardinality of J
$\mathcal{K}$	Unit set indexed by k, with the cardinality of K

VARIABLES

ρ_t	RSS at timeslot t
ρ^{Agg}	DRSS
P_t^R	Integrated RES at timeslot t in the whole system
R	Daily integrated RES in the whole system

L_t	Load at timeslot t in the whole system
$P_{k,t}^G$	Power generation of unit k at timeslot t
$P_{k,t}^{Gup}$	Upward reserve offered by unit k at timeslot t
$P_{k,t}^{Gdn}$	Downward reserve offered by unit k at timeslot t
$x_{k,t}$	Commitment state of unit k at timeslot t (binary variable)
$SC_{k,t}$	Star-up cost of unit k at timeslot t
$LP_{j,t}^*$	The jth typical load profile after DR (multiple plans for customers)
$u_{j,t}^{max}, u_{j,t}^{min}, v_{j,t}, \lambda_j$	Dual variables
G^{max}	Peak value of the aggregated unit generation
G^{Avg}	Average value of the aggregated unit generation
t_{peak}	Time slot when unit generation is maximal
t_{valley}	Time slot when unit generation is minimal
$t_{Rup1/2}$	Successive timeslots when the ramp-up rate of units is maximal
$t_{Rdn1/2}$	Successive timeslots when the ramp-down rate of units is maximal

PARAMETERS

$\rho^{Agg.max}$	Maximal available DRSS (M-DRSS)
R^{max}	Maximal aggregated daily MW value of RES
L	Daily aggregated load
a_k, b_k, c_k	Cost coefficients of unit k
c_k^{up}, c_k^{dn}	Price for upward/downward reserve of unit k
W_t^{up}, W_t^{dn}	Upward/downward reserve requirement
ψ	Curtailment price of RES
$P_{i,t}^L$	Load of customer i at timeslot t
$LP_{i,t}$	Load profile of customer i at timeslot t
$LP_{j,t}$	Typical load profile j at timeslot t
α_i	RSC of customer i (evaluated in hindsight)
π	Retail price
L_i^{Day}	Daily consumption of customer i
$P_k^{G.max}$	Upper power generation limit of unit k
$P_k^{G.min}$	Lower power generation limit of unit k
$X_{k,t-1}^{ON/OFF}$	ON/OFF time of unit k at timeslot t-1
$T_k^{ON/OFF}$	Minimal ON/OFF time of unit k
$ramp_k$	Ramping rate of unit k
P_t^{L0}	Inflexible load at timeslot t
L_j^{Day}	Daily consumption of typical load profile j
δ_j	Tolerance of comfort loss for typical load profile j

I. INTRODUCTION

Achieving widespread use of renewable energy sources (RES) is one of the most important targets of future power systems [1], [2]. Due to the intermittent and volatile characteristics of RES, it is too costly or even infeasible to balance the power supply and demand by only relying on the conventional units under significant RES penetration. Curtailments of RES will occur if the flexibility of the conventional units is not sufficient to compensate for the fluctuations in the RES. For instance, in 2016, China curtailed 49.7 TWh of wind power, with a national average curtailment rate of 17.1% [3].

The *demand response* (DR) has been widely studied to help integrate RES [4]–[8]. Its applications include, but are not limited to, frequency regulation, ramping or following reserves, additional unit commitment, and load reshaping or shifting [7], [8]. In this paper, the DR is studied as an approach to reshape the load curve to *reduce the burden of power balancing for conventional units* (such as ramping, valley demand, and peak demand) and to facilitate integration of a significant amount of RES.

Current DR programs can be categorized into price-based DR (PDR) and incentive-based DR (IDR) [9]. Various PDR programs have been studied, such as [10]–[13], where customers' load profiles are controlled indirectly by price signals sent by the DR providers. Although the local marginal pricing (LMP) has been widely used in the wholesale market, customers on the retail side are risk-aware to be exposed to wholesale dynamic price. Many recent studies (e.g., [9], [14], and [15]) have examined the potential obstacles of PDRs when deployed on a large scale. In practice, the retail price for residential customers cannot be directly adjusted by the utilities in countries or regions where the electricity market has not been in operation. Thus, in this paper, we focus on IDR, where the retail prices require no changes and customers face a flat retail price, similar to a the scheme in [9].

To ensure the performance of a DR program, two crucial issues should be resolved: how to evaluate a customer's performance in the DR and how to operate the DR resources [16]. The former issue determines the objectives of customers who reshape their load profiles and obtain the corresponding rewards, while the latter issue focuses on designing an effective DR scheme to induce customers to reshape their loads curves.

Although considerable work has been performed regarding DR and RES integration, there remains no method for the direct evaluation of the *renewable energy share of a customer's daily electricity consumption* (RSC). It is difficult to quantify different customers' real contributions to the amount of integrated renewable energy, which will result in the unfairness and ineffectiveness of the DR and hinder the deployment and promotion of DR programs.

To address these problems, this paper aims to determine i) how to evaluate the RSC and ii) how to design an efficient scheme to help customers increase the RSC through the DR and accordingly facilitate integrating RES in the whole system.

A. FIRST CONTRIBUTION AND ITS RELATED WORK

In the current IDR, the methods for evaluation of the customers' DR performances are not related to the customers'

real contributions to the integrated RES, while the customer baseline load (CBL) is widely used [16]–[20]. The CBL denotes a predicted load curve in the absence of a DR event, and the difference between a customer's actual load after the DR and the CBL is regarded as the contribution of the customer. We argue that the CBL-based method faces *two potential problems*.

The first problem is determining how to calculate the CBL accurately and efficiently for numerous DR customers. One of the most widely used CBL calculation methods is the *HighX* of *Y* method adopted by the PJM, New York ISO, and California ISO [16]. In [18], three metrics, the mean absolute error, the bias, and the overall performance index, were used to assess the *HighX* of *Y* CBL, and the results belied substantial inherent inaccuracies that could not be ignored. However, the improved methods based on regression or clustering are too complicated to be used in practice due to their heavy computational burdens, especially when the DR is deployed on a large scale [19]. Meanwhile, some customers are capable of strategically adjusting their CBL to acquire high rewards, which is called the ''moral hazard'' problem [20]. In addition, the CBLs must be calculated in a centralized form according to orders such as the Federal Energy Regulatory Commission's (FERC) order 745, which was related to incentives and put considerable pressure on the data storage and computation requirements of the DR provider [20].

The second problem is that CBL-based methods only focus on the load curtailment quantity but ignore the different impacts on the amount of integrated RES of different load profiles, failing to link the customers' responses with their real contributions to the objective of the DR program, i.e., increasing the renewable energy share of the whole system. In practice, a greater power balancing burden is put on the conventional units, and the curtailment of the RES is also more likely to occur when the aggregated load is inconsistent with the maximal available RES than when the aggregated load is always synchronous with the available RES. In particular, if two customers have heterogeneous load profiles, they will have different impacts on the profile of the aggregated load, thereby resulting in different amounts of integrated RES. Therefore, even if the first problem, i.e., the CBL's calculation, is solved by improving the existing algorithms, then the second problem will not be addressed unless a novel evaluation method is adopted.

Except for the CBL-based methods, some researchers have also considered directly providing the desired load profiles as the load reshaping objective to customers without using the CBL [14], [15], [21]. The calculation problem of the CBL can be approached to some extent, but it remains unclear how customers impact the RES integration. To analyze a customer's impact on some system-level features, the *marginal impact* on system-level features of the load profiles was proposed [22] and is adopted in this paper. However, the focus in the previous study [22] was on the optimal retail rate but not RES integration.

To solve the DR performance evaluation problem, we propose a method for calculating the *marginal impact of a customer on the amount of integrated RES* in the whole system (MIR). We then prove the MIR is reasonable to evaluate the *renewable energy share of a customer's daily consumption* (RSC). The concept and evaluation method of MIR and RSC are the first contribution of this paper and they are both proposed for the first time in the researches of power systems.

As a metric for DR performance evaluation, the RSC can solve the potential problems of the CBL-based method summarized above, while it bridges the real contribution of a customer in the DR program. Moreover, to numerically validate the proposed evaluation methods, several kinds of the marginal impacts on the power balancing burden for conventional units caused by a customer (MIBs) were tested in the case study.

B. SECOND CONTRIBUTION AND ITS RELATED WORK

Based on the first contribution, the proposed RSC will be tailored in the DR program. Thus, we present an RSC-based DR which is defined as one that provides an incentive to customers to increase the RSC by reshaping their load profiles, which accordingly increases the amount of integrated RES in the whole system. How to induce massive customers to increase their RSC is also the second work of this paper.

Current DR schemes can be categorized into two types, depending on whether the customers are passively scheduled or if they actively make decisions. In the first type, several DR customers are aggregated, modeled as a virtual power plant (VPP), and dispatched in the unit commitment [23], optimal power flow [24], and frequency regulation [25]. This approach is easily deployed in practice. However, it does not represent a user-friendly approach because it is difficult to ensure utilities for the customers, especially for residential customers. In the second type, customers can control the tradeoff between the reward and comfort loss to maximize their utilities. Interactions between the DR providers and customers are often included in these schemes due to coupled dependent variables in the model. For instance, in [9] and [17], customers could continuously adjust the load reduction according to the coupon (incentive) level until convergence. Also, in another literature [26], the interactions between customers were studied from a game perspective. Compared with the above VPP-based schemes, customers could individually make optimal decisions. However, it is not practical to interact with numerous customers frequently due to potential challenges, such as the process being too complex for residents [27] and communication reliability problems [28].

Recent surveys on the retail market have found that customers prefer to follow principles such as multi-options that are utilized successfully in the customer-centric IT industry [29]. In the PDR program, customized retail prices have been studied based on the consumption regularity of customers, where multi-price plans have been designed [30]. Meanwhile, the energy-aware demand-side recommendation

systems have been studied to help customers choose a suitable plan from the customized plans [27], [31]. In this way, frequent interactions between customers and the DR providers can be avoided, while customers can also make optimal decisions. However, similar techniques are not applicable to the IDR because there is no direct metric to evaluate the DR performance on the integrated RES. The RSC proposed in this paper can play that role.

As a result, *the second contribution of this paper is a novel DR scheme to facilitate the integration of RES in the whole system by increasing the renewable energy share of customers' consumption* (RSC). In this scheme, frequent interactions are avoided, while customers can make a customized choice. To obtain multiple reshaped load profiles that can help customers increase their RSC, a bilevel optimization problem is modeled and converted to a mathematical program with primal and dual constraints (MPPDC). A case study shows that the proposed scheme considerably reduces the power balancing burden for conventional units and prevents the curtailment of RES accordingly.

The remainder of the paper is organized as follows. A method for calculating the MIR and RSC is presented in Section II. In Section III, the proposed RSC is tailored in DR programs, and the RSC-based DR scheme is introduced. A case study and analysis are shown in Section IV. Finally, conclusions and future research are provided in Section V.

II. MIR AND RSC

A. PRELIMINARIES

Before evaluating the RSC, we first study three metrics that can be easily derived based on measurements. For an independent power system, we define the renewable energy share of the system-level consumption (RSS) as the ratio between the integrated RES and the total load at timeslot t. The RSS is denoted by ρ_t and calculated as follows:

$$\rho_t = \frac{P_t^R}{L_t} \times 100\% \quad \forall t \tag{1}$$

where P_t^R and L_t are the MW magnitudes of integrated RES and load in the entire system at timeslot t, respectively. Let $\mathcal{T} := \{1, 2, \ldots, T\}$ denote a set of time index. For the sake of simplicity, $\forall t$ denotes $\forall t \in \mathcal{T}$ in this paper, and similar notation is used throughout the paper. In addition to the RSS, the daily renewable energy share of the system-level consumption (DRSS) is defined as the fraction of the daily integrated RES and load, denoted by R and L, respectively. Let ρ^{Agg} denote the DRSS, thus it is determined by:

$$\rho^{Agg} = \frac{R}{L} = \frac{\sum_{t \in \mathcal{T}} P_t^R}{\sum_{t \in \mathcal{T}} L_t} = \frac{\sum_{t \in \mathcal{T}} \rho_t L_t}{\sum_{t \in \mathcal{T}} L_t} \times 100\%. \tag{2}$$

Except for these two system-level indexes, we subsequently define an individual-level metric, i.e., the load profile. Let $\mathcal{I} := \{1, 2, \ldots, I\}$ collect a set of customer index, and we calculate a customer's load profile as follows:

$$LP_{i.t} = \frac{P_{i.t}^L}{\sum_{t \in \mathcal{T}} P_{i.t}^L} \quad \forall i, \forall t \tag{3}$$

where $P_{i.t}^L$ and $LP_{i.t}$ denote the kW magnitude of load and the load profile of customer i at timeslot t, respectively. It is not difficult to get a remark that the load profiles for any given customer sum to unity over the course of a day i.e., $\sum_{t \in \mathcal{T}} LP_{i.t} = 1$.

The above-mentioned metrics, including load profile, RSS and DRSS are the bases for our further study about the evaluation of RSC. In practice, although the actual integrated RES depends on the system's operation status and is unknown in advance, it can be measured in *hindsight*, and the RSS and DRSS can be calculated accurately based on measurements, as shown in the upper left side of Fig. 1. Similarly, each customer's load profile can be obtained by smart meters easily, as shown in the upper right side of Fig. 1. However, our goal is to get the RSC, i.e., the lower left side of Fig. 1. Note that the RSC cannot be directly measured due to a lack of power tracing of the RES for customers. Thus, our work in this section is to investigate a reasonable method to map the measured system- and individual-level knowledge to an evaluation metric, i.e., RSC.
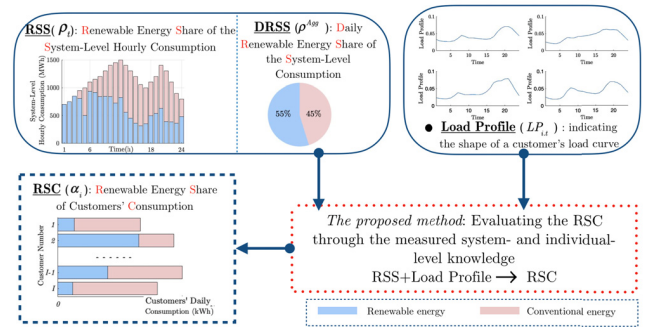

FIGURE 1. Relationship between RSS, DRSS, load profile and RSC.

Before continuing to investigate the RSC, we need to claim that when it comes to a DR program (increasing the RSC) but not only evaluation, the scheduling should be completed beforehand instead of relying on measurements in hindsight. Thus, in Section III, the load service entity (LSE) will be considered. Generally, the LSE has the ability to mimic the ISO's day-ahead unit commitment (UC) and predict the RSS and DRSS, which have been widely used in DR schemes [9], [17]. Meanwhile, the load profile is treated as a control variable. The DR scheme considers day-ahead predictions will be illustrated in detail in Section III, while the next two subsections continue to focus on the evaluation method of RSC.

B. MIR

As mentioned above, our work is to map the RSS and load profiles to the RSC, namely the lower right red frame in Fig. 1. Since the power tracing to the end-customers is impractical, we will investigate the RSC evaluation method from the perspective of the customers' impact and contribution to the amount of integrated RES.

To quantify the impact of a load profile on the system's operation status, the concept of *marginal impact* is leveraged.

We can represent the system load L_t and customer i's load profile $LP_{i,t}$ respectively as vectors $\vec{L}$ and $\vec{LP}_i$, where the relevant vector space is spanned by the timeslots and has the cardinality of T as its dimension. Because we assess the impact on RES integration from demand sides, we assume the supply-side settings have been given. Then, we can consider a function $f.(\vec{L})$ which denotes a system-level feature of interest (for example, $f_R(\vec{L})$ denotes the daily integrated RES, and $f_{PVD}(\vec{L})$ denotes the peak/valley difference [32]) and depends on the entirety of the daily system load. Although we do not know the explicit structure of $f.(\vec{L})$, the abstract function form is sufficient for further study. Note that $f.(\vec{L})$ can be treated as continuous over a small domain, similar to the study of marginal system-cost impact presented previously [22].

To determine the marginal impact of a given customer i's usage on that system-level feature function we consider the result of a small perturbation to that customer's load which preserves that customer's load profile. Such a perturbation must take the form $P_{i,t}^L \longrightarrow P_{i,t}^L + (\Delta P)LP_{i,t}$, where ΔP is a small amount of energy. The system load is thereby perturbed by the same amount, so that $L_t \longrightarrow L_t + (\Delta P)LP_{i,t}$ or in equivalent vector notation as $\vec{L} \longrightarrow \vec{L} + (\Delta P)\vec{LP}_i$. The marginal impact of the perturbation on the function $f.(\vec{L})$ is defined as the ratio of the corresponding perturbation on the function $f.(\vec{L})$ divided by ΔP in the limit that ΔP vanishes,

$$F_i = \lim_{\Delta P \to 0} \frac{f.[\vec{L} + (\Delta P)\vec{LP}_i] - f.(\vec{L})}{\Delta P} \quad (4)$$

Roughly speaking, we proportionally allocate a very small increment (ΔP) to the original load of customer i based on his load profile and subsequently calculate the marginal change in index $f.(\vec{L})$ at the system level, and the result accordingly represents the marginal impact of this customer on the given system-level feature.

In the evaluation, we have two types of system-level features. The first one is the daily integrated RES for the whole system, which corresponds to a customer's marginal impact on the amount of integrated RES (MIR). The second type is a set of features that reflects the extent of the power balancing burden on the units, such as the demand peak, peak/valley difference, and ramping rate. These correspond to the respective marginal impacts on the power balancing burden for units caused by a customer (MIBs). The MIR directly quantifies the contribution of a customer to the integrated RES, while the MIBs indirectly impact the integrated RES from multiple dimensions. As a result, the MIR is studied in detail and used to evaluate the RSC in this section, while MIBs are used to validate the evaluation results in the case study (Section IV), while they are detailed in the Appendix.

Based on the definition of marginal impact described above and Equation (4), the MIR of customer i is defined as the instantaneous change in the daily integrated RES (R) when the customer increases his load but maintains the same load profile. Thus, $f.(\vec{L})$ in Equation (4) is detailed by $f_R(\vec{L})$,

and F_i represents MIR_i. Following the definition above, we can get that $MIR_i = \lim_{\Delta P \to 0} \frac{f_R[\vec{L} + (\Delta P)\vec{LP}_i] - f_R(\vec{L})}{\Delta P}$. For further derivation, we assume the RSS after the perturbation, i.e., ρ_t, is the same as that in the previous perturbation, which means the generation structure does not change in the perturbation process. The assumption can hold because ΔP is very small. Because $f_R(\vec{L})$ denotes the daily integrated RES, it can be calculated as a sum of each timeslot's product of the RSS and the MW magnitude of the system load, i.e., $f_R(\vec{L}) = \sum_{t \in \mathcal{T}} \rho_t L_t$. Concurrently, the daily integrated RES after the perturbation holds a similar structure, i.e., $f_R[\vec{L} + (\Delta P)\vec{LP}_i] = \sum_{t \in \mathcal{T}} [\rho_t(L_t + \Delta P \cdot LP_{i,t})]$. Therefore, the MIR can be calculated as follows:

$$
\begin{aligned}
MIR_i &= \lim_{\Delta P \to 0} \frac{f_R[\vec{L} + (\Delta P)\vec{LP}_i] - f_R(\vec{L})}{\Delta P} \\
&= \lim_{\Delta P \to 0} \frac{\sum_{t \in \mathcal{T}} [\rho_t(L_t + \Delta P \cdot LP_{i,t})] - \sum_{t \in \mathcal{T}} (\rho_t L_t)}{\Delta P} \\
&= \lim_{\Delta P \to 0} \frac{\sum_{t \in \mathcal{T}} (\rho_t \Delta P \cdot LP_{i,t})}{\Delta P} = \sum_{t \in \mathcal{T}} \rho_t LP_{i,t} \quad \forall i
\end{aligned}
$$

(5)

Thus, the MIR can be regarded as a weighted average of the RSS, where the weight coefficients are the proportion of each timeslot's demand to the daily total demand, i.e., the load profile. Note that the RSS and the customer's load profile both affect his MIR. The RSS is determined by the system operation status, where the capability of the units and the profile of available RES play the leading roles. Therefore, given a certain system status, i.e., the RSS, a customer's contribution to the integrated RES is determined by his load profile.

C. RENEWABLE ENERGY SHARE OF A CUSTOMER'S CONSUMPTION (RSC)

Based on the quantified contribution to the integrated RES of each customer, i.e., MIR, the RSC can be evaluated.

Assumption: The *loss* in the transmission or distribution is not considered in the evaluation. If taking the *loss* into account, we can regard it as a virtual consumer and evaluate it with other real customers jointly. However, as the ratio between the loss and total load is relatively small [33], the loss is assumed to be negligible.

Because the RSC is the percentage of a customer's daily consumption that can be reasonably attributed to the RES, several conditions should be satisfied:

1) Let α_i be the evaluated RSC of customer i, then $\alpha_i \in [0, 1]$ since it is a percentage.

2) If $MIR_i \neq 0$ and $MIR_j \neq 0$, then $\frac{\alpha_i}{\alpha_j} = \frac{MIR_i}{MIR_j}$. Evaluating the RSC is a profit allocation problem, and allocating in proportion to the marginal impact, i.e., MIR, denotes a fair allocation method. Namely, the evaluation of RSC should be proportional to each customer's MIR, while there exists the same proportional coefficient for all the customers.

3) The sum of the RES consumption of all the customers should be equal to the integrated RES at the system level:

$$\sum_{i \in \mathcal{I}} \left(\alpha_i \sum_{t \in \mathcal{T}} P_{i,t}^L \right) = R \qquad (6)$$

There exists a unique solution that satisfies all the conditions above, and it is given by $\alpha_i = MIR_i$.

Proof: Because of the second condition, we can write $\alpha_i = \theta MIR_i$, where the coefficient θ is the common ration of α_i and MIR_i. Replacing α_i with $\theta MIRI_i$ on the left side of Equation (6) yields the following:

$$
\begin{aligned}
&\sum_{i \in \mathcal{I}} \left(\alpha_i \sum_{t \in \mathcal{T}} P_{i,t}^L \right) \\
&= \sum_{i \in \mathcal{I}} \left(\theta MIR_i \sum_{t \in \mathcal{T}} P_{i,t}^L \right) \\
&= \sum_{i \in \mathcal{I}} \left(\theta \sum_{t \in \mathcal{T}} (\rho_t LP_{i,t}) \sum_{t \in \mathcal{T}} P_{i,t}^L \right) \\
&= \theta \sum_{i \in \mathcal{I}} \sum_{t \in \mathcal{T}} \left(\rho_t LP_{i,t} \sum_{t \in \mathcal{T}} P_{i,t}^L \right) \\
&= \theta \sum_{i \in \mathcal{I}} \sum_{t \in \mathcal{T}} \left(\rho_t \frac{P_{i,t}^L}{\sum_{t \in \mathcal{T}} P_{i,t}^L} \sum_{t \in \mathcal{T}} P_{i,t}^L \right) \\
&= \theta \sum_{t \in \mathcal{T}} \sum_{i \in \mathcal{I}} \rho_t P_{i,t}^L = \theta \sum_{t \in \mathcal{T}} \rho_t \sum_{i \in \mathcal{I}} P_{i,t}^L = \theta \sum_{t \in \mathcal{T}} \rho_t L_t = \theta R.
\end{aligned}
\qquad (7)
$$

The unique solution that satisfies Equation (6), and therefore condition 3), is $\theta = 1$. Furthermore, since $0 \le MIR_i \le 1$, condition 1 is automatically satisfied when $\theta = 1$. As a result, $\alpha_i = MIR_i$ is the unique solution that satisfies all the necessary conditions of the RSC.

In conclusion, the resultant RSC evaluation approach, i.e., $\alpha_i = MIR_i = \sum_{t \in \mathcal{T}} \rho_t LP_{i,t}$, converted the system- and individual-level measurement-based indices, the RSS and load profile, to an evaluation index, RSC, as shown as Fig. 1.

Intuitively, the percentage of energy that can be treated as coming from RES for a customer depends on the RES performance in the whole system together with the shape of his load curve. The evaluation can be performed in *hindsight* without any RES and load forecasting, which means that the evaluation result will not be affected by prediction errors. However, if customers want to obtain a higher RSC, the most direct way is to reshape his load profile according to the RSS. Thus, the system operation states should be predicted beforehand. To address this problem, a bilevel optimization model that accounts for upward/downward reserves to compensate for the RES and load stochastic fluctuations (prediction errors) will be presented in the next section.

III. RSC-BASED DR SCHEME
The contribution of each customer to the amount of integrated RES can be quantitatively evaluated based on the above method. In this section, we will present a novel DR scheme to motivate customers to obtain a higher RSC, which accordingly facilitates the integration of the RES.

A. ASSUMPTIONS
In the proposed scheme, the following assumptions are made:

1) The LSE has the ability to mimic the ISO's day-ahead UC and predict the available RSS, similar to DR schemes reported previously [9] [17]. Simultaneously, the upward and downward reserve requirements are incorporated in the optimization model to compensate for stochastic fluctuations (prediction errors) of the RES and load [33].

2) Considering climate change, the energy shortage, and sustainability in future energy systems, integrating as many RES as possible will be the final solution to these challenges and will be significantly more economical than using conventional energy [1]. Thus, in the cost function of the UC model, i) the capital and generation cost of RES is negligible, and ii) the penalty for curtailment of the RES is included [33], and iii) the monetary incentive given to customers to facilitate the integration of RES is neglected.

3) The customers who participate in the DR program are rational and will increase the RSC by choosing a reshaped load profile to follow from the multi-plan that is most similar to the original load profile because it brings the smallest comfort loss. Customers behaviors with bounded rationality are left for future study.

B. RSC-BASED DR
1) INCENTIVE
The RSC can directly evaluate the contribution to the integrated RES of a customer, and thus, the RSC-based DR is defined as follows. To integrate more RES in the entire system, the DR provider motivates customers to reshape their load profiles to obtain a higher RSC by giving an incentive, such as an electric bill discount. Customers with a higher RSC will obtain a higher incentive rate. The incentive rate is discussed, but the absolute incentive value is not, because the absolute incentive value is also related to the daily consumption. The discount rate a customer can receive is a monotonically increasing function of his RSC, such as linear, quadratic, or exponential function. For the sake of simplicity, we use the linear form in this paper, defined as Equation (8). When it comes to other forms, the customer's response model introduced in Section III.C needs to be modified as a consequence, while further discussions about the different incentive functions will be studied in the future.

$$D_i(\alpha_i) = \kappa \alpha_i \qquad (8)$$

In the incentive function, κ is a positive coefficient and $\kappa \alpha_i$ is the discount rate the customer can receive, which is proportional to his RSC. Let π denote the retail price and L_i^{Day} denote the daily consumption of customer i, then the actual monetary incentive the customer can get is $\kappa \alpha_i (\pi L_i^{Day})$. Note that the setpoint of the proportional coefficient κ is adjustable for the DR providers but will not influence the result of our model in this paper.

The advantages of the RSC-based DR are as follows:
(1) The CBL-based method in the DR is replaced by the RSC, which means the inaccuracy, the centralized calcula-

tion, and the moral hazard problems are all avoided. According to Equation (5), all the variables of the RSC can be measured but not forecasted. Although the DR scheme introduced in the next subsection is also based on some predicted information, the final evaluation and reward are based on measurements without predictions.

(2) The DR performance and the corresponding reward allocation are related to the MIR, which represents the greatest equity method.

2) DEPLOYMENT

Under the proposed scheme, DR customers are motivated to obtain a higher RSC to receive more incentive. Considering the structure of the RSC evaluation method, customers can increase their RSC by reshaping their load profiles to better match the RSS while being subject to some physical constraints.

However, the RSS is unknown for customers in advance, and it depends on the system operation status. In general, the LSE will link the customers and the DR providers and provide a professional DR service. As described in the first section, customers, especially residents, prefer to follow multi-options [29]. Following this perspective, we require the LSE to provide multiple RSC-increasing plans to allow the customers to choose the most convenient one. Multi-plans are *multiple reshaped load profiles that can increase the RSC*.

To obtain these reshaped load profiles, the LSE will formulate an optimization model. Nevertheless, the dimensionality of the optimization model will be a significant challenge if we incorporate all the customers' load profiles into the model. Due to the structure of the MIR and RSC (Eq.(5)), two customers who share the same load profile must have the same RSC because the RSS is unique for the entire system, while the RSC is related to the load profiles but not related to the load level. Thus, in lieu of applying every customers' load profile, clustered typical load profiles are applied in our model. Many researchers have proposed various approaches for clustering [30], [31], [35]. Therefore, the LSE is only required to design the optimal RSC-increasing plans for these clustered typical profiles and publish the plans to the demand side. The customer's HEMS will choose the most convenient one to follow by scheduling flexible loads and his own distributed energy resources.

Human behaviors are not the focuses of this paper. Assumption (3) in Section III.A ensures that customers will rationally reshape their load profile following the RSC-increasing plans in the DR. Thus, problems such as a customer's irregular behavior are not considered.

C. MULTI-PLANS FOR INCREASING RSC

In this subsection, we formulate a bilevel optimization problem to address how to obtain multiple RSC-increasing plans.

Firstly, at the upper level, the LSE mimics the ISO's day-ahead unit commitment to decide the RSS at each timeslot based on an optimization model similar to those reported previously [33], [34]. Therefore, the upper-level model, denoted as $\mathcal{P}1$. Because all the notations used in the model are tabled and described before the Section I and are general in many similar researches, we do not introduce them in detail here.

$$\min_{\Xi^{UC}} C = \sum_{k \in \mathcal{K}} \sum_{t \in T} [a_i(P_{k.t}^G)^2 + b_i P_{k.t}^G + c_i x_{k.t}$$
$$+ SC_{k.t} + c_i^{up} P_{k.t}^{Gup} + c_i^{dn} P_{k.t}^{Gdn} +$$
$$\psi \left(P_t^{R.\max} - \rho_t L_t \right)] \tag{9a}$$

$$SC_{k.t} = \max\{0, \ x_{k.t}(1 - x_{k.t-1})\} \ \forall t \in \mathcal{T}_{-1}, \ \forall k \tag{9b}$$

$$x_{k.t} P_k^{G.\max} \le P_{k.t}^G \le x_{k.t} P_k^{G.\max} \quad \forall t, \ \forall k \tag{9c}$$

$$\left| P_{k.t}^G - P_{k.t-1}^G \right| \le ramp_k \quad \forall t \in \mathcal{T}_{-1}, \ \forall k \tag{9d}$$

$$(X_{k.t-1}^{ON} - T_k^{ON})(x_{k.t-1} - x_{k.t}) \ge 0 \quad \forall t \in \mathcal{T}_{-1}, \ \forall k \tag{9e}$$

$$(X_{k.t-1}^{OFF} - T_k^{OFF})(x_{k.t} - x_{k.t-1}) \ge 0 \quad \forall t \in \mathcal{T}_{-1}, \ \forall k \tag{9f}$$

$$\sum_{k \in \mathcal{K}} P_{k.t}^{Gup} \ge W_t^{up} \quad \forall t \tag{9g}$$

$$P_{k.t}^{Gup} \ge 0 \quad \forall t, \ \forall k \tag{9h}$$

$$\sum_{k \in \mathcal{K}} P_{k.t}^{Gdn} \ge W_t^{dn} \quad \forall t \tag{9i}$$

$$P_{k.t}^{Gdn} \ge 0 \quad \forall t, \ \forall k \tag{9j}$$

$$P_{k.t}^G + P_{k.t}^{Gup} \le x_{k.t} P_k^{G.\max} \quad \forall t, \ \forall k \tag{9k}$$

$$P_{k.t}^G - P_{k.t}^{Gdn} \ge x_{k.t} P_k^{G.\min} \quad \forall t, \ \forall k \tag{9l}$$

$$P_{k.t}^G + P_{k.t}^{Gup} - P_{k.t-1}^G \le ramp_k \quad \forall t \in \mathcal{T}_{-1} \ \forall k \tag{9m}$$

$$P_{k.t}^G - P_{k.t}^{Gdn} - P_{k.t-1}^G \ge -ramp_k \quad \forall t \in \mathcal{T}_{-1} \ \forall k \tag{9n}$$

$$0 \le \rho_t L_t \le P_t^{R.\max} \quad \forall t \tag{9o}$$

$$\sum_{k \in \mathcal{K}} P_{k.t}^G = (1 - \rho_t) L_t \quad \forall t \tag{9p}$$

$$L_t = \sum_{j \in \mathcal{J}} \sum_{t \in \mathcal{T}} L_j^{Day} \cdot LP_{j.t}^* + P_t^{L0} \quad \forall t \tag{9q}$$

$$x_{k.t} = \{0, 1\} \quad \forall t \ \forall k \tag{9r}$$

The objective of this model is to minimize the total cost, which is composed of the generation and start-up costs of the conventional units, upward and downward reserve costs offered by the units, and the cost of RES curtailment. The optimization variable set is expressed as: $\Xi^{UC} = \left\{ x_{k.t}, P_{k.t}^G, \rho_t, SC_{k.t}, P_{k.t}^{Gup}, P_{k.t}^{Gdn} \right\}$. The start-up cost is defined by Equation (9b). The constraints include the maximal and minimal power output, ramping rate, and minimal ON/OFF times, which are given by Equations (9c)–(9f). To compensate for stochastic fluctuations (prediction errors) of the RES and load, the upward and downward reserves, i.e., $P_{k.t}^{Gup}$ and $P_{k.t}^{Gdn}$, should be provided by the units. Therefore, Equations (9g)–(9n) describe constraints on the reserve offered by each unit. Note that each unit's reserve at timeslot

t is treated as an optimization variable for better minimizing total cost. Equation (9o) shows the upper and lower bounds of the actual integrated RES. Furthermore, Equation (9p) defines the power balance equality constraint. Equation (9q) shows the MW value of a load at timeslot t. The available RES output and the aggregated daily consumption of each typical load profile together with the inflexible load are both assumed to be forecasted, while the prediction errors can be compensated by the upward and downward reserves. Note that $LP^*_{j.t}$ is the optimization variable in the lower-level model.

The lower-level problem denoted as $\mathcal{P}2$ is modeled for every RSC-increasing plan, namely, to optimize the load profiles to get higher RSC. As a customer, the objective function is to minimize the electricity bill minus the incentive in the DR:

$$\min \quad \pi L_i^{Day} - \kappa \alpha_i \left(\pi L_i^{Day} \right) \tag{10}$$

We only reshape the load shape but do not increase or decrease the daily consumption, i.e., L_i^{Day} is not an optimization variable. Therefore, the objective can be translated to *maximize the RSC*. Additionally, as mentioned in Section III.B, two customers who share the same load profile must have identical RSC. Therefore, a lower-level model is formulated for each clustered typical load profile in lieu of formulating a model every customer, i.e., for $\forall j \in \mathcal{J}$:

$$\max_{LP^*_{j.t}} \sum_{t \in \mathcal{T}} \rho_t LP^*_{j.t} \tag{11a}$$

$$\sum_{t \in \mathcal{T}} LP^*_{j.t} = 1 : \lambda_j \tag{11b}$$

$$LP^*_{j.t} \geq (1 - \delta_j) LP_{j.t} : \mu^{\min}_{j.t} \quad \forall t \tag{11c}$$

$$LP^*_{j.t} \leq (1 + \delta_j) LP_{j.t} : \mu^{\max}_{j.t} \quad \forall t \tag{11d}$$

$$(LP^*_{j.t} - LP^*_{j.t-1})(LP_{j.t} - LP_{j.t-1}) \geq 0 : v_{j.t} \; \forall t \in \mathcal{T}_{-1} \tag{11e}$$

The objective function given by (11a) is converted from Equation (10). Equation (11b) shows that the daily electricity consumption will not change after a DR, which means the RSC increase arises only from the load profile reshaping and not the load consumption curtailment or incentive. The comfort loss tolerance (δ_j) is between 0 and 1. Therefore, Equations (11c) and (11d) define the regulation range constraint at timeslot t. A larger δ_j implies that there are more load flexibilities but also results in more comfort loss to the customers. Equation (11e) indicates that the trends of any two successive timeslots should be the same as the original one, and thus, the reshaping will not undermine the original behavior.

D. ALGORITHM
A bilevel optimization problem is formulated by $\mathcal{P}1$ and $\mathcal{P}2$ defined above. We transform it into single-level mixed-integer linear programming (MILP), which can be solved efficiently.

1) MPPDC
The lower-level optimization problem, i.e., $\mathcal{P}2$, is a linear programming problem (LP), so its Karush-Kuhn-Tucker (KKT) conditions are necessary and sufficient. There are two approaches to convert a bilevel problem into a single-level problem. The first one is to recast the lower level problem, i.e., $\mathcal{P}2$, as its KKT condition and adding it to the upper-level problem, i.e., $\mathcal{P}1$, as a set of additional complimentary constraints, which is known as a mathematical program with equilibrium constraints (MPEC) approach [17], [36]. Another approach is based on the primal-dual approach and formulates the bilevel problem as a mathematical program with primal and dual constraints (MPPDC) [37], [38]. Generally, the MPPDC approach can avoid complementarity and slackness constraints that must be solved by the *big-M* approach in the MPEC, and thus, it presents a smaller computational burden [38]. Therefore, we adopt the MPPDC approach in this paper.

The MPPDC approach consists of replacing the lower-level problem, i.e., $\mathcal{P}2$, by its primal constraints, which are defined by Equations (11b)–(11e), the dual constraints given by Equations (12)–(14), and the strong duality equality given by Equation (15):

$$-\rho_t - \lambda_j + \mu^{\max}_{j.t} - \mu^{\min}_{j.t} = 0 \quad t = 1, \forall j, \tag{12}$$

$$-\rho_t - \lambda_j + \mu^{\max}_{j.t} - \mu^{\min}_{j.t} - v_{j.t}(LP_{j.t} - LP_{j.t-1}) = 0$$
$$\forall t \in \mathcal{T}_{-1}, \forall j \tag{13}$$

$$\mu^{\min}_{j.t}, \mu^{\max}_{j.t}, v_{j.t} \geq 0 \quad \forall t, \forall j, \tag{14}$$

$$\sum_{t \in \mathcal{T}} \rho_t LP^*_{j.t} + \lambda_j - \sum_{t \in \mathcal{T}} \mu^{\max}_{j.t}(1 + \delta_j) LP_{j.t}$$
$$+ \sum_{t \in \mathcal{T}} \mu^{\min}_{j.t}(1 - \delta_j) LP_{j.t} = 0 \quad \forall j \tag{15}$$

Further details about the MPPDC can be found elsewhere [38]. Aside from the constraints of the MPDDC approach, additional constraints should also be included to ensure the RSC of all the typical load profiles will increase:

$$\sum_{t \in \mathcal{T}} \rho_t LP^*_{j.t} \geq \alpha_j \quad \forall j \tag{16}$$

The LSE will mimic the ISO's day-ahead unit commitment to obtain the RSS, as mentioned in Section III.A, while the RSC before the DR in Equation (16) can be obtained accordingly.

Following the above procedure, the equivalent single-level optimization problem denoted by $\mathcal{P}3$ is formulated as follows:

$$\min_{\Xi^{UC}, \Xi^{Dual}, LP^*_{j.t}} C \tag{17a}$$

$$\begin{cases} \text{Eq.}(9b) \sim \text{Eq. (9r)}, \quad \text{Eq.}(11b) \sim \text{Eq. (11e)} \\ \text{Eq. (12)} \sim Eq. \text{ (15)} \\ \text{Eq. (16)} \end{cases} \tag{17b}$$

where $\Xi^{Dual} = \left\{ \lambda_j, u^{max}_{j.t}, u^{min}_{j.t}, v_{j.t} \right\}$ denotes a set of dual variables, Equations (9b)–(9r) define the primal constraints of the upper-level problem, Equations (11b)–(11e) define

the primal constraints of the lower-level problem, Equations (12)–(15) define the dual constraints and strong duality equality used to convert a bilevel problem into a single-level problem, and Equation (16) defines the additional constraints.

2) LINEARIZATION

Although the bi-level problem is accurately converted to a single-level problem, $\mathcal{P}3$ can still not be readily processed due to the bilinear product terms $\rho_t LP_{j.t}^*$ in Equations (15) and (16). Therefore, we employ the binary expansion method [36] to linearize these terms. We use 2^Z discrete points to approximate possible values of ρ_t in its feasible interval [0, 1]:

$$\rho_t = \Delta\rho_t \cdot \sum_{z=1}^{Z} 2^{z-1} u_{t.z} \quad \forall t, \tag{18}$$

where $u_{t.z}, z = 1, 2, \ldots, Z$ are the auxiliary binary variables that control the approximate value of ρ_t, and the step size $\Delta\rho_t$ is given as $\frac{1}{2^Z}$. ρ_t in the bilinear product term can be replaced by the right side of Equation (18):

$$\rho_t LP_{j.t}^* = \Delta\rho_t \cdot \sum_{z=1}^{Z} 2^{z-1} LP_{j.t}^* u_{t.z} \quad \forall t, \forall j. \tag{19}$$

Letting $LP_{j.t}^* u_{t.z} = q_{j,t,z}, z = 1, 2, \cdots, Z$, Equation (19) can be converted to Equation (20a), with extra constraints given by (20b) and (20c):

$$\rho_t LP_{j.t}^* = \Delta\rho_t \cdot \sum_{z=1}^{Z} 2^{z-1} q_{j.t.z} \quad \forall t, \forall j, \tag{20a}$$

$$0 \le LP_{j.t}^* - q_{j.t.z} \le (1 + \delta_j)LP_{j.t}(1 - u_{t.z}) \forall t, \forall j, \forall z \tag{20b}$$

$$0 \le q_{j.t.z} \le (1 + \delta_j)LP_{j.t} u_{t.z} \quad \forall t, \forall j, \forall z. \tag{20c}$$

Two extra constraints are used to ensure that $q_{j.t.z} = 0$ when $u_{t.z} = 0$ and $q_{j.t.z} = LP_{j.t}$ when $u_{t.z} = 1$. Details are provided elsewhere [36].

Except for the bilinear product terms, the generation cost of units is a quadratic function, and the constrained cost variable (CCV) method is utilized to segmentally linearize it [39]. Note that both binary expansion method and CCV method have been proved to be accurate and efficient [36], [39]. As a consequence, $\mathcal{P}3$ is transformed into the MILP based on the MPPDC and accurate linearization, which can be solved by various solvers, such as GUROBI and Cplex.

IV. CASE STUDY

In this section, we test and validate the RSC and run the RSC-based DR program on the generated test system.

A. SIMULATION SETUP

First, the test system was generated. For the customers, we used a large number of residential load curves provided by OpenEI [40] and clustered them using the *k*-means algorithm [35]. Fifteen typical load profiles were generated. The daily consumption was set to 20,000 MWh. Without loss of generality, the daily consumption of all typical loads was set to be the same. Data from 10 units were taken from a previous

report [42]. The upward and downward reserve requirements for the whole system represented 10% of the available RES at each timeslot, and the reserve price offered by each generating unit was assumed to be 10% of the marginal generation cost of the last segment. Each typical load's tolerance of the comfort loss (δ_j) was initially set to 0.2 and sampled from 0.1 to 0.3 in the latter test. In the binary expansion method, Z was set to 11, and thus, we used $2^{11} = 2048$ discrete points to approximate the value of ρ_t.

For the RES data, we normalized the solar and wind power curves of the PJM [41] collected on July 2nd, 2017 and used them to obtain the basic trend of the maximal available RES output in our test system. The maximal available DRSS (M-DRSS) were sampled from 10% to 70%, and the daily maximal available RES output was determined as follows: $R^{max} = \rho^{Agg.Max} L$. Seven available RES curves were generated and are shown in Fig. 2. Aside from a certain RES profile with various M-DRSS, we also adopted the RES profiles on the 2nd of each month in 2017 and specified that the M-DRSS at 60% generated 12 different available RES curves, as shown in Fig. 3.
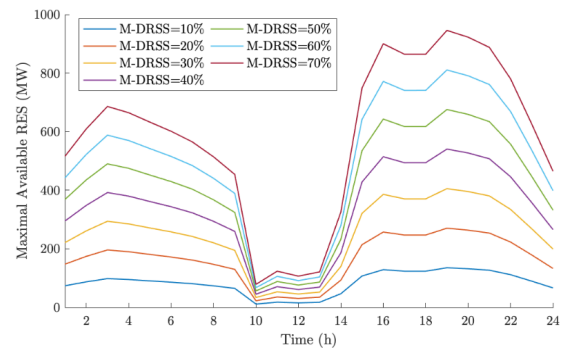

FIGURE 2. Seven available RES curves with different M-DRSS values based on a certain RES profile.
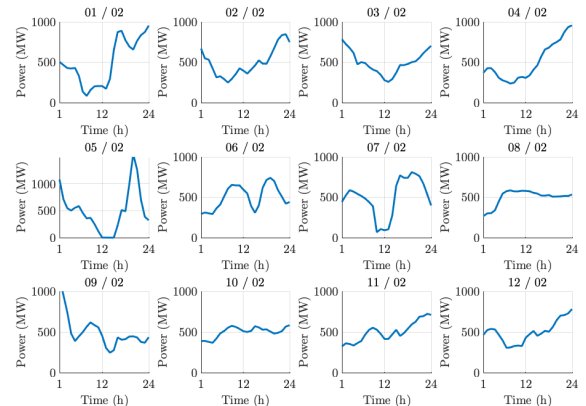

FIGURE 3. Twelve available RES curves with the M-DRSS fixed at 60% based on 12 different RES profiles.

B. MARGINAL IMPACTS ON THE POWER BALANCING BURDEN FOR UNITS

Before running our model, some MIBs were defined to validate our test results. As is introduced in Section II,

a customer whose RSC is higher should have lower MIBs than a customer with a lower RSC. Therefore, based on four typically used quantitative power-balancing burden indices, the peak-to-average ratio (PAR) [43], peak/valley load difference (PVD) [32], maximal ramp-up rate (Rup), and maximal ramp-down rate (Rdn), four MIBs can be derived based on the definition of marginal impact and Equation (4), where $f.(\vec{L})$ is denoted by PAR, PVD, Rup, and Rdn, as shown in Equations (21a)–(21d). Furthermore, the DRSS was also considered, and the marginal impact on the DRSS was derived as Equation (21e). The derivation processes of each MIB is provided in the Appendix.

Note that smaller values for the first four indices correspond to fewer balancing burdens for the units, while a larger value of MI_{DRSS} corresponds to a more integrated RES.

$$MIB_{PAR} = \frac{TG^{Avg}LP_{j.t_{peak}} - G^{max}}{T \cdot (G^{Avg})^2} \tag{21a}$$

$$MIB_{PVD} = LP_{j.t_{peak}} - LP_{j.t_{valley}} \tag{21b}$$

$$MIB_{Rup} = |LP_{j.t_{Rup2}} - LP_{j.t_{Rup1}}| \tag{21c}$$

$$MIB_{Rdn} = |LP_{j.t_{Rdn2}} - LP_{j.t_{Rdn1}}| \tag{21d}$$

$$MI_{DRSS} = \sum_{t \in \mathcal{T}} \rho_t LP_{j.t} - \rho^{Agg} \tag{21e}$$

C. RSC EVALUATION TEST AND ANALYSIS

We evaluated the RSC of 15 typical load profiles in the M-DRSS range of 10–70% with a certain RES profile, i.e., the RES curves in Fig. 2. Fig. 4 shows the RSC of all the typical load profiles, and several key observations were made. First, the DRSS equaled the M-DRSS when their values were not very large, which means that there was no RES curtailment because the balancing burden for the units was not severe. However, when the M-DRSS increased to 40%, the DRSS was less than the M-DRSS, which means that curtailment of the RES occurred. Second, the RSCs of some load profiles were clearly higher than those of others. For instance, customer type-15 obtained the highest RSC, while customer type-12 obtained the lowest. Meanwhile, the difference in the customers' RSCs increased with the M-DRSS. The RSCs of some customers, such as type-15, were higher than the M-DRSSs. This occurred because some customers had significantly lower RSC, e.g., customer type-12. Thus, the renewable energy share of some customers was occupied by others due to different contributions to the integrated RES. If these customers want to increase their RSC, they must reshape their load profiles.

In addition to the observations above, we also found that when the RES profile is specified, the rank of RSC of these 15 typical load profiles did not change significantly with increasing M-DRSS. Overall, regardless of the M-DRSS, customers who shared load profile type-15 were always evaluated as good customers that facilitated integrating the RES, but type-12 had a negative impact on RES integration. Alternatively, we can specify a certain M-DRSS but adopt different RES profiles, i.e., the RES curves in Fig. 3, as a further test. Fig. 5 shows the RSC evaluation results of two
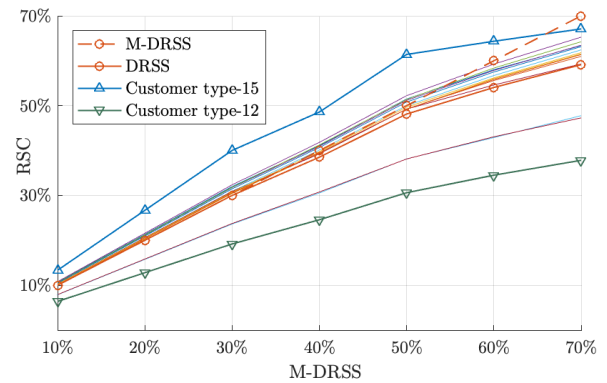

FIGURE 4. RSC of 15 typical load profiles under different M-DRSS.
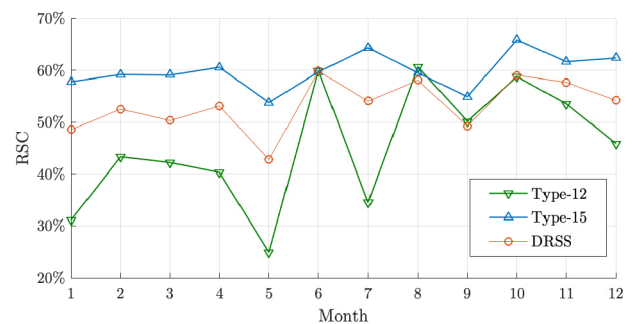

FIGURE 5. RSC of typical load profiles with different RES profiles.

representative types of loads, type-12 and type-15, and the DRSS. Although type-15 obtained a higher RSC than type-12 in most months, in agreement with the cases when the RES profile was specified, there were several irregular results, such as in June and August. Also, both the RSC and DRSS fluctuate over the 12 different RES profiles. The reason is that the evaluation of RSC depends not only on the load profile but also the RSS, which is related to system-level RES output. When a load profile approximated the RES profile, it was more likely to obtain a higher RSC. Thus, when we adopted different RES profiles to test the RSC of each load type, we cannot assert which customer will always get higher RSC. For instance, type-12 obtained an RSC higher than that of type-15 in June and August. Intuitively, the test results in Fig. 4 and Fig. 5 obey the mathematical structure of the proposed evaluation method.

D. VALIDATION OF RSC

The previous subsection showed the evaluation results of the RSC. To validate the RSC evaluation results analytically and numerically, in this section we show detailed operation states and the results of several MIBs defined in Section IV.B.

First, the operation states of the whole system with the maximal available RES output from Fig. 2 at an M-DRSS of 60% were simulated, and they are shown in Fig. 6, while typical type-15 and type-12 load profiles are shown in Fig. 7. An extreme ramp-up rate was required between timeslots 9 to 10,
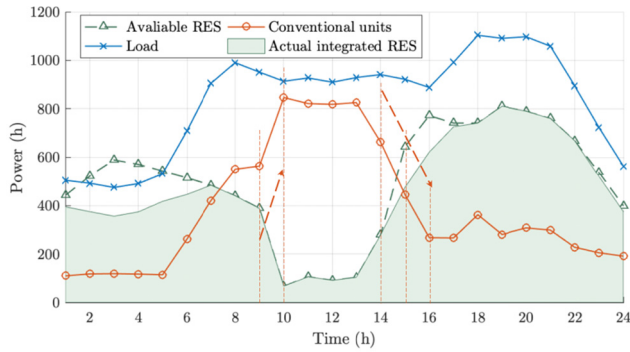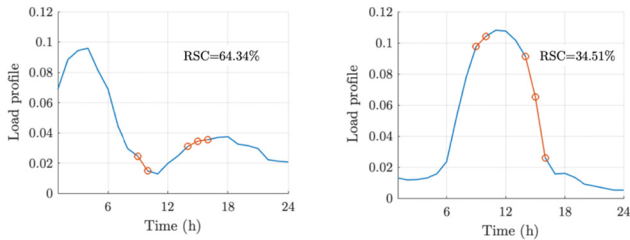
FIGURE 6. Operation states of the whole system.

FIGURE 7. Load profiles of type-15 and type-12 (left-15 and right-12).

FIGURE 8. Radar charts of the MIBs at different M-DRSS magnitudes.

while an extreme ramp-down rate was required between timeslots 14 to 16, where the curtailment of the RES occurred due to insufficient ramping capacities of the units. Type-12 was evidently more responsible for these ramping events, while type-15 experienced a positive impact on preserving ramping flexibility. Meanwhile, the RES was adequate between timeslots 1 and 6 and curtailment occurred. The peak for type-15 also occurred during these timeslots. Conversely, the peak load of type-12 occurred between timeslots 10 and 13, but the RES was not adequate. As a result, when more customers were sharing the load profiles, such as type-15 but not type-12, a reduced power balancing burden was placed on the units, and the RES would be better integrated.

To quantitatively validate our RSC evaluation results, MIB_{PAR}, MIB_{PVD}, MIB_{Rup}, MIB_{Rdn}, and MI_{DRSS} were introduced above. Four maximal available RES output curves in Fig. 2 with the M-DRSS samples of 20%, 40%, 60%, and 70% are tested, successively. The five indices for type-15 and type-12, and the average value of 15 load profiles are shown in Fig. 8. For a more intuitive representation, the axis representing MI_{DRSS} is reversely plotted, so an outside circle (a larger circle) indicates a worse impact on the power balancing and integration of the RES. Based on the presented results, the following observations were made. First, type-15 performed better than type-12 under different M-DRSS conditions, since the blue circle is always larger than the red circle. Type-15 exhibited a negative marginal impact on the first four power balancing burden indices, i.e., PAR, PVD, Rup, and Rdn, which means the generation capacities and ramping of units were reduced for type-15. Type-15 also
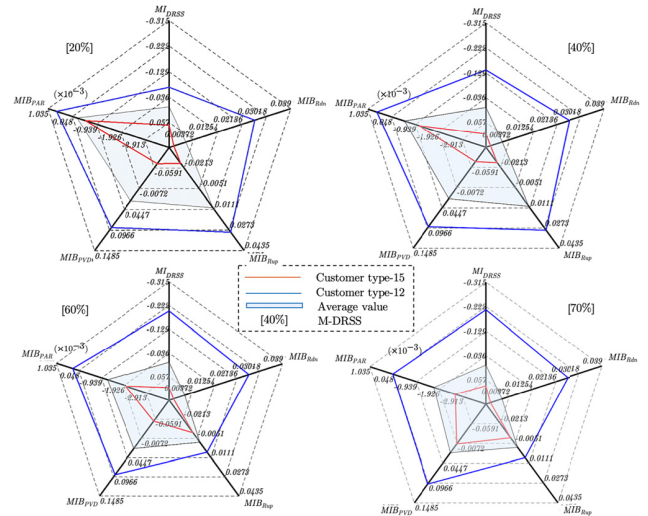
had a positive impact on the DRSS, which facilitated greater RES integration. Conversely, a larger power balancing burden occurred when customers shared the load profile, such as type-12. The five indices for verification matched the RSC evaluation results.

In this subsection, the evaluation results of the RSC were validated through the analysis of operation states and several MIBs indices. Thus, our proposed evaluation method is corroborated to be reasonable.

### E. RSC-BASED DR TEST AND ANALYSIS

In practice, not all the customers will take part in the DR. Therefore, the DR participation percentage was defined before running the DR program as the ratio between DR customers' daily consumption and the total load daily consumption in the whole system.

$$DR\% = \sum_{j \in \mathcal{J}} L_j^{Day}/L \times 100\%. \qquad (22)$$

We adopt the maximal available output curve in Fig. 2 with M-DRSS=60%. The RSC-based DR program is run with $DR\%$ setting to be 60%. The 15 typical load profiles and their reshaped load profiles after the DR, i.e., multi plans, are shown in Fig. 9. Because of the physical constraints in the model, the load profiles after the DR did not change significantly, and the rhythm was also maintained. Additionally, the RSC values for all typical load profiles increased after the DR, as shown in the brackets in Fig. 9. From the perspective of the system, the RSC-based DR could reduce the power balancing burden for conventional units and facilitate the integration of additional RES. As shown in Table 1, PAR, PVD (MW), Rup (MW), and Rdn (MW) all decreased after the DR. Meanwhile, the DRSS increased from 54.05% to 57.54%, which means that 418.8 MWh of RES curtailment was avoided because the amount of available RES was 12,000 MWh. Meanwhile, the total operation cost of the

TABLE 1. Five system-level features before and after the DR.

	PAR	PVD	Rup	Rdn	DRSS
without DR	2.209	736.28	283.28	215.89	54.05%
with DR	2.104	634.95	207.93	215.31	57.54%
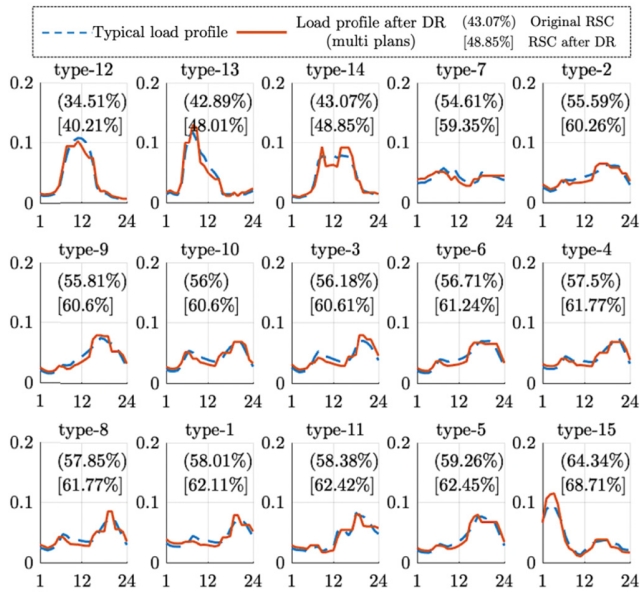
FIGURE 9. Load profiles before and after the DR with the RSC.

FIGURE 10. Impact of the DR percentage on integrated RES.

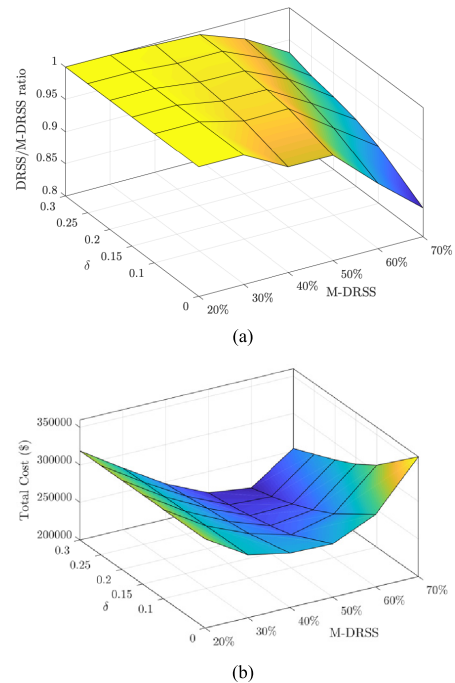**FIGURE 11.** Impact of the comfort loss tolerance on integrated RES.

units (except the curtailment cost) in the whole system also decreased from \$225,148 to \$202,416. This result was due not only to more integrated RES but also to fewer regulating requirements for the units.

Then, we tested the impact of the DR participation percentage and comfort loss tolerance δ on the RES integration and total cost. The ratio of the DRSS to the M-DRSS was used to evaluate the integration performance, which was expected to approach 1. The M-DRSS varied from 20% to 70%. For the case presented in Fig. 10, the comfort loss tolerance was set to 0.2 while the DR participation percentage changed from 0 to 100%. Furthermore, the DR participation percentage was fixed at 60% but δ changed from 0 to 0.3. The results are shown in V. Both the DR percentage and δ represented a positive DR level, where the larger value of the former indicated that more customers were responsive to the RSC-based DR, while a more significant value of the latter indicated a more flexible load.

The following observations were made. First, under a certain DR participation percentage or δ, the DRSS/M-DRSS ratio decreased with the increase in the M-DRSS (See Fig. 10 (a) and V (a)). This occurred because the ramping or regulation capacities of the units were insufficient to integrate all the available RES when the M-DRSS was high. Thus, a curtailment of some RES was necessary to ensure the reliability of the power systems. Meanwhile, the total cost

decreased with the increase in the M-DRSS at the beginning, because more RES was integrated whose generation costs were negligible. However, when the RES penetration was significant (more than 50%), the total cost increased with the increase in the M-DRSS (See Fig. 10 (b) and V (b)). The reason is that the curtailment of the RES occurred, and

$$MIB_{PAR} = \lim_{\Delta P \to 0} \frac{f_{PAR}(\vec{L} + \Delta P \cdot \vec{LP}_j) - f_{PAR}(\vec{L})}{\Delta P}$$

$$= \lim_{\Delta P \to 0} \frac{\frac{G^{max} + \Delta P \cdot LP_{j.t_{peak}}}{G^{Avg} + \Delta P/T} - \frac{G^{max}}{G^{Avg}}}{\Delta P}$$

$$= \lim_{\Delta P \to 0} \frac{TG^{Avg}LP_{j.t_{peak}} - G^{max}}{T \cdot (G^{Avg})^2 + \Delta P \cdot G^{Avg}} = \frac{TG^{Avg}LP_{j.t_{peak}} - G^{max}}{T \cdot (G^{Avg})^2} \tag{24a}$$

$$MIB_{PVD} = \lim_{\Delta P \to 0} \frac{f_{PVD}(\vec{L} + \Delta P \cdot \vec{LP}_j) - f_{PVD}(\vec{L})}{\Delta P}$$

$$= \lim_{\Delta P \to 0} \frac{(G_{t_{peak}} + \Delta P \cdot LP_{j.t_{peak}}) - (G_{t_{valley}} + \Delta P \cdot LP_{j.t_{valley}}) - (G_{t_{peak}} - G_{t_{valley}})}{\Delta P}$$

$$= LP_{j.t_{peak}} - LP_{j.t_{valley}} \tag{24b}$$

$$MIB_{Rup} = \lim_{\Delta P \to 0} \frac{f_{Rup}(\vec{L} + \Delta P \cdot \vec{LP}_j) - f_{Rup}(\vec{L})}{\Delta P}$$

$$= \lim_{\Delta P \to 0} \frac{|(G_{t_{Rup2}} + \Delta P \cdot LP_{j.t_{Rup2}}) - (G_{t_{Rup1}} + \Delta P \cdot LP_{j.t_{Rup1}})| - |G_{t_{Rup2}} - G_{t_{Rup1}}|}{\Delta P}$$

$$= |LP_{j.t_{Rup2}} - LP_{j.t_{Rup1}}| \tag{24c}$$

$$MIB_{Rdn} = \lim_{\Delta P \to 0} \frac{f_{Rdn}(\vec{L} + \Delta P \cdot \vec{LP}_j) - f_{Rdn}(\vec{L})}{\Delta P}$$

$$= \lim_{\Delta P \to 0} \frac{|(G_{t_{Rdn2}} + \Delta P \cdot LP_{j.t_{Rdn2}}) - (G_{t_{Rdn1}} + \Delta P \cdot LP_{j.t_{Rdn1}})| - |G_{t_{Rdn2}} - G_{t_{Rdn1}}|}{\Delta P}$$

$$= |LP_{j.t_{Rdn2}} - LP_{j.t_{Rdn1}}| \tag{24d}$$

$$MI_{DRSS} = \lim_{\Delta P \to 0} \frac{f_{DRSS}(\vec{L} + \Delta P \cdot \vec{LP}_j) - f_{DRSS}(\vec{L})}{\Delta P}$$

$$= \lim_{\Delta P \to 0} \frac{\frac{\sum_{t \in \mathcal{T}} \rho_t(L_t + \Delta P \cdot \vec{LP}_j)}{L + \Delta P} - \frac{\sum_{t \in \mathcal{T}} \rho_t L_t}{L}}{\Delta P}$$

$$= \lim_{\Delta P \to 0} \frac{L \sum_{t \in \mathcal{T}} \rho_t L_t - \sum_{t \in \mathcal{T}} \rho_t L_t}{L(L + \Delta P)}$$

$$= \sum_{t \in \mathcal{T}} \rho_t L_t - \frac{\sum_{t \in \mathcal{T}} \rho_t L_t}{L} = \sum_{t \in \mathcal{T}} \rho_t L_t - \rho^{Agg} \tag{24e}$$

the curtailment cost played a crucial role in the total cost. Furthermore, more reserve was required for the uncertainty of the RES when the M-DRSS was high, and the reserve cost increased. Thus, significant RES penetration is environmentally friendly, but the curtailment of RES is difficult to avoid.

However, the RSC-based DR facilitated integrating considerably more RES in the whole system while reducing the total cost. Furthermore, a larger DR participation percentage and δ both facilitated the performance of the DR. For instance, when the M-DRSS was 70%, the DRSS/M-DRSS ratio increased from less than 0.85 to about 0.95 with the DR participation percentage increasing (See Fig. 10 (a)). Meanwhile, the total cost decreased from \$359,982 to \$253,508 (See Fig. 10 (b)). Thus, a fraction of the operation cost saving can be allocated to DR customers for incentive. When the M-DRSS was low (about 20%), the RSC-based DR performance was not evident, because all the RES could

be integrated by relying on conventional units. Therefore, for a DR provider, attracting more customers to join to the RSC-based DR program or giving more rewards to some customers to obtain a larger tolerance of comfort loss are two useful approaches for integrating more RES. Meanwhile, in practice, the RSC-based DR is more necessary with significant RES penetration.

V. CONCLUSION

In this paper, we addressed two crucial issues of the DR: performance evaluation and deployment scheme. For the evaluation, the MIR of a customer was proposed and proven to be reasonable for evaluating the RSC. The CBL was replaced by the RSC to directly evaluate customers' contributions to the integrated RES and the performance in the DR. An RSC-based DR scheme was also proposed, where customers were motivated to reshape their load profiles to

obtain a higher RSC, which contributed to the reduction of the power balancing burden for conventional units and integration of more RES. We corroborated the evaluation method analytically and numerically, while the DR program performed well on integrating considerably more RES into the power system.

The limitations of the proposed method are as follows. First, the network constraints were not considered. Additionally, customers' decisions with bounded rationality were also ignored. As a result, future work will focus on a more comprehensive MIR evaluation method and the DR scheme will account for customers' behaviors.

APPENDIX
We will show how to obtain the MIBs in Section IV.

First, we leverage several system-level metrics to evaluate the power balancing burden of units and performance of RES integration.

1) Peak-to-average ratio (PAR) [43]:

$$f_{PAR}(\overrightarrow{L}) = \frac{G^{max}}{G^{Avg}} \tag{23a}$$

where G^{max} and G^{avg} denote the peak and average value of the aggregated generation of units, respectively.

2) Peak/valley difference (PVD) [32],

$$f_{PVD}(\overrightarrow{L}) = G_{t_{peak}} - G_{t_{valley}} \tag{23b}$$

where t_{peak} and t_{valley} are the timeslots when the peak and valley value of the aggregated generation of units occur. $G_{t_{peak}}$ and $G_{t_{valley}}$ are the magnitudes of generation at t_{peak} and t_{valley}, respectively.

3) Maximal ramp-up rate (Rup):

$$f_{Rup}(\overrightarrow{L}) = |G_{t_{Rup1}} - G_{t_{Rup2}}| \tag{23c}$$

where t_{Rup1} and t_{Rup2} are two successive timeslots when the ramp-up rate of the aggregated generation of units is maximal. $G_{t_{Rup1}}$ and $G_{t_{Rup2}}$ are the magnitudes of generation at t_{Rup1} and t_{Rup2}, respectively.

4) Maximal ramp-down rate (Rdn)

$$f_{Rdn}(\overrightarrow{L}) = |G_{t_{Rdn1}} - G_{t_{Rdn2}}| \tag{23d}$$

where t_{Rdn1} and t_{Rdn2} are two successive timeslots when the ramp-down rate of the aggregated generation of units is maximal. $G_{t_{Rdn1}}$ and $G_{t_{Rdn2}}$ are the magnitudes of generation at t_{Rdn1} and t_{Rdn2}, respectively.

5) Daily RSS (DRSS)

$$f_{DRSS}(\overrightarrow{L}) = \frac{\sum\limits_{t \in \mathcal{T}} \rho_t L_t}{L} \tag{23e}$$

Then, we can obtain the corresponding Marginal Impacts Indexes on corresponding system-level metrics based on the definition of *marginal impact*, i.e., Eq. (4), (24a)–(24e), as shown at the top of the previous page.

REFERENCES
[1] J. Li, F. Liu, Z. Li, C. Shao, and X. Liu, "Grid-side flexibility of power systems in integrating large-scale renewable generations: A critical review on concepts, formulations and solution approaches," *Renew. Sustain. Energy Rev.*, vol. 93, pp. 272–284, Oct. 2018.

[2] L. Che, X. Liu, X. Zhu, M. Cui, and Z. Li, "Assessment of dispatch intervals in power systems with high wind penetration," *IEEE Trans. Sustain. Energy*, to be published.

[3] C. Dong, Y. Qi, W. Dong, X. Lu, T. Liu, and S. Qian, "Decomposing driving factors for wind curtailment under economic new normal in China," *Appl. Energy*, vol. 217, pp. 178–188. May 2018.

[4] H. Han, S. Gao, Q. Shi, H. Cui, and F. Li, "Security-based active demand response strategy considering uncertainties in power systems," *IEEE Access*, vol. 5, pp. 16953–16962, 2017.

[5] Q. Shi, C.-F. Chen, A. Mammoli, and F. Li, "Estimating the profile of incentive-based demand response (IBDR) by integrating technical models and social-behavioral factors," *IEEE Trans. Smart Grid*, to be published.

[6] Q. Hu, F. Li, X. Fang, and L. Bai, "A framework of residential demand aggregation with financial incentives," *IEEE Trans. Smart Grid*, vol. 9, no. 1, pp. 497–505, Jan. 2018.

[7] C. Chen, M. Cui, X. Wang, K. Zhang, and S. Yin, "An investigation of coordinated attack on load frequency control," *IEEE Access*, vol. 6, pp. 30414–30423, 2018.

[8] J. Aghaei and M.-I. Alizadeh, "Demand response in smart electricity grids equipped with renewable energy sources: A review," *Renew. Sustain. Energy Rev.*, vol. 18, pp. 64–72, Feb. 2013.

[9] H. Zhong, L. Xie, and Q. Xia, "Coupon incentive-based demand response: Theory and case study," *IEEE Trans. Power Syst.*, vol. 28, no. 2, pp. 1266–1276, May 2013.

[10] W. Wei, F. Liu, and S. Mei, "Energy pricing and dispatch for smart grid retailers under demand response and market price uncertainty," *IEEE Trans. Smart Grid*, vol. 6, no. 3, pp. 1364–1374, May 2015.

[11] Z. Chen, L. Wu, and Y. Fu, "Real-time price-based demand response management for residential appliances via stochastic optimization and robust optimization," *IEEE Trans. Smart Grid*, vol. 3, no. 4, pp. 1822–1831, Dec. 2012.

[12] R. Li, Q. Wu, and S. S. Oren, "Distribution locational marginal pricing for optimal electric vehicle charging management," *IEEE Trans. Power Syst.*, vol. 29, no. 1, pp. 203–211, Jan. 2014.

[13] S. Fan, Z. Li, J. Wang, L. Piao, and Q. Ai, "Cooperative economic scheduling for multiple energy hubs: A bargaining game theoretic perspective," *IEEE Access*, vol. 6, pp. 27777–27789, 2018.

[14] C. Chen, J. Wang, and S. Kishore, "A distributed direct load control approach for large-scale residential demand response," *IEEE Trans. Power Syst.*, vol. 29, no. 5, pp. 2219–2228, Sep. 2014.

[15] S. Fan, G. He, K. Jia, and Z. Wang, "A novel distributed large-scale demand response scheme in high proportion renewable energy sources integration power systems," *Appl. Sci.*, vol. 8, no. 3, p. 452, 2018.

[16] T. K. Wijaya, M. Vasirani, and K. Aberer, "When bias matters: An economic assessment of demand response baselines for residential customers," *IEEE Trans. Smart Grid*, vol. 5, no. 4, pp. 1755–1763, Jul. 2014.

[17] X. Fang, Q. Hu, F. Li, B. Wang, and Y. Li, "Coupon-based demand response considering wind power uncertainty: A strategic bidding model for load serving entities," *IEEE Trans. Power Syst.*, vol. 31, no. 2, pp. 1025–1037, Mar. 2016.

[18] S. Mohajeryami, M. Doostan, and P. Schwarz, "The impact of Customer Baseline Load (CBL) calculation methods on Peak Time Rebate program offered to residential customers," *Electr. Power Syst. Res.*, vol. 137, pp. 59–65, Aug. 2016.

[19] Y. Zhang, W. Chen, R. Xu, and J. Black, "A cluster-based method for calculating baselines for residential loads," *IEEE Trans. Smart Grid*, vol. 7, no. 5, pp. 2368–2377, Sep. 2016.

[20] S. Mohajeryami, M. Doostan, A. Asadinejad, and P. Schwarz, "Error analysis of customer baseline load (CBL) calculation methods for residential customers," *IEEE Trans. Ind. Appl.*, vol. 53, no. 1, pp. 5–14, Jan./Feb. 2017.

[21] A. Safdarian, M. Fotuhi-Firuzabad, and M. Lehtonen, "Optimal residential load management in smart grids: A decentralized framework," *IEEE Trans. Smart Grid*, vol. 7, no. 4, pp. 1836–1845, Jul. 2016.

[22] Y. Yu, G. Liu, W. Zhu, F. Wang, B. Shu, K. Zhang, N. Astier, and R. Rajagopal, "Good consumer or bad consumer: Economic information revealed from demand profiles," *IEEE Trans. Smart Grid*, vol. 9, no. 3, pp. 2347–2358, May 2018.

[23] Y. Sun, Z. Chen, Z. Li, W. Tian, and M. Shahidehpour, "EV charging schedule in coupled constrained networks of transportation and power system," *IEEE Trans. Smart Grid*, vol. 10, no. 5, pp. 4706–4716, Sep. 2019.

[24] W. Shi, N. Li, C.-C. Chu, and R. Gadh, "Real-time energy management in microgrids," *IEEE Trans. Smart Grid*, vol. 8, no. 1, pp. 228–238, Jan. 2017.

[25] Y. Zhou, M. Cheng, and J. Wu, "Enhanced frequency response from industrial heating loads for electric power systems," *EEE Trans. Ind. Informat.*, vol. 15, no. 6, pp. 3388–3399, Jun. 2019.

[26] P. Srikantha and D. Kundur, "Resilient distributed real-time demand response via population games," *IEEE Trans. Smart Grid*, vol. 8, no. 6, pp. 2532–2543, Nov. 2017.

[27] F. Luo, G. Ranzi, X. Wang, and Z. Y. Dong, "Social information filtering-based electricity retail plan recommender system for smart grid end users," *IEEE Trans. Smart Grid*, vol. 10, no. 1, pp. 95–104, Jan. 2019.

[28] K. Jia, G. He, S. Fan, G. Lin, S. Lu, and F. Pan, "Cyber and physical integration analysis for automated residential demand response in smart grid," in *Proc. IEEE PES Asia–Pacific Power Energy Eng. Conf.*, Nov. 2017, pp. 1–6.

[29] T. Chen, Q. Alsafasfeh, H. Pourbabak, and W. Su, "The next-generation U.S. retail electricity market with customers and Prosumers—A bibliographical survey," *Energies*, vol. 11, no. 1, p. 8, 2017.

[30] J. Yang, J. Zhao, F. Wen, and Z. Y. Dong, "A framework of customizing electricity retail prices," *IEEE Trans. Power Syst*, vol. 33, no. 3, pp. 2415–2428, May 2018.

[31] Y. Zhang, K. Meng, W. Kong, and Z. Y. Dong, "Collaborative filtering-based electricity plan recommender system," *EEE Trans. Ind. Informat.*, vol. 15, no. 3, pp. 1393–1404, Mar. 2019.

[32] S. Wang, N. Zhang, Z. Li, and M. Shahidehpour, "Modeling and impact analysis of large scale V2G electric vehicles on the power grid," in *Proc. IEEE PES Innov. Smart Grid Technol.*, Tianjin, China, May 2012, pp. 1–6.

[33] P. Li, D. Yu, M. Yang, and J. Wang, "Flexible look-ahead dispatch realized by robust optimization considering CVaR of wind power," *IEEE Trans. Power Syst.*, vol. 33, no. 5, pp. 5330–5340, Sep. 2018.

[34] J. Wang, M. Shahidehpour, and Z. Li, "Security-constrained unit commitment with volatile wind power generation," *IEEE Trans. Power Syst.*, vol. 23, no. 3, pp. 1319–1327, Aug. 2008.

[35] J. Kwac, J. Flora, and R. Rajagopal, "Household energy consumption segmentation using hourly data," *IEEE Trans. Smart Grid*, vol. 5, no. 1, pp. 420–430, Jan. 2014.

[36] R. Li, W. Wei, S. Mei, Q. Hu, and Q. Wu, "Participation of an energy hub in electricity and heat distribution markets: An MPEC approach," *IEEE Trans. Smart Grid*, vol. 10, no. 4, pp. 3641–3653, Jul. 2019.

[37] C. Zhang, Q. Wang, J. Wang, P. Pinson, J. M. Morales, and J. Østergaard, "Real-time procurement strategies of a proactive distribution company with aggregator-based demand response," *IEEE Trans. Smart Grid*, vol. 9, no. 2, pp. 766–776, Mar. 2018.

[38] J. M. Arroyo, "Bilevel programming applied to power system vulnerability analysis under multiple contingencies," *IET Generat., Transmiss. Distrib.*, vol. 4, no. 2, pp. 178–190, Feb. 2010.

[39] R. D. Zimmerman, C. E. Murillo-Sánchez, and R. J. Thomas, "MATPOWER: Steady-state operations, planning, and analysis tools for power systems research and education," *IEEE Trans. Power Syst.*, vol. 26, no. 1, pp. 12–19, Feb. 2011.

[40] *Commercial and Residential Hourly Load Profiles for all TMY3 Locations in the United States*. Accessed: Oct. 11, 2018. [Online]. Available: https://openei.org/doe-opendata/dataset/commercial-and-residential-hourly-load-profiles-for-all-tmy3-locations-in-the-united-states

[41] *Data Miner 2-PJM*. Accessed: Oct. 11, 2018. [Online]. Available: http://dataminer2.pjm.com/list

[42] C.-P. Cheng, C.-W. Liu, and C.-C. Liu, "Unit commitment by Lagrangian relaxation and genetic algorithms," *IEEE Trans. Power Syst.*, vol. 15, no. 2, pp. 707–714, May 2000.

[43] Y. Zhou, R. Kumar, and S. Tang, "Incentive-based distributed scheduling of electric vehicle charging under uncertainty," *IEEE Trans. Power Systems*, vol. 34, no. 1, pp. 3–11, Jan. 2019.

SHUAI FAN (S'18) is currently pursuing the Ph.D. degree with Shanghai Jiao Tong University. His research interests include economic operation, demand response, and online optimization in electric power systems.

ZHENGSHUO LI (S'12–M'16) received the bachelor's and Ph.D. degrees from the Department of Electrical Engineering, Tsinghua University, Beijing, China, in 2011 and 2016, respectively. He was a Postdoctoral Fellow with the Tsinghua–Berkeley Shenzhen Institute (TBSI), from 2016 to 2018. He is currently a Professor with Shandong University, Jinan, Shandong, China. His research interests include economic dispatch and security analysis of transmission and distribution grids and demand response in smart grids. He was a recipient of the Best Paper Award of 2015 China National Doctoral Academic Annual Meeting, the Best Paper of 2016 IEEE PES General Meeting, and the Excellent Doctoral Dissertation Award of Tsinghua University, in 2016. He was also a recipient of the Best Reviewer Award for the IEEE TRANSACTIONS ON SMART GRID, in 2015 and the *Proceedings of CSEE*, in 2017 and 2018. His dissertation was selected for Springer Theses.

ZUYI LI (SM'09) received the B.S. and M.S. degrees from Shanghai Jiao Tong University, Shanghai, China, in 1995 and 1998, respectively, and the Ph.D. degree from the Illinois Institute of Technology (IIT), Chicago, in 2002, all in electrical engineering. He is currently a Professor with the Electrical and Computer Engineering Department, Illinois Institute of Technology (IIT). His research interests include economic and secure operation of electric power systems, cyber security in smart grid, renewable energy integration, and the electric demand management of data centers.

GUANGYU HE (M'04–SM'15) received the B.S. degree in automation and the Ph.D. degree in electrical engineering from Tsinghua University, Beijing, China, in 1994 and 1999, respectively, where he joined the Department of Electrical Engineering, in 1999. In 2014, he joined the School of Electronic Information and Electrical Engineering, Shanghai Jiao Tong University, Shanghai, China, where he is currently a Professor. His research interests include power systems analysis and operations, demand response, machine learning, and nonlinear optimization for large-scale problems.

• • •